Journal of Applied Sciences

ISSN 1812-5654

science alert

ANSInet
an open access publisher
http://ansinet.com

Journal of Applied Sciences 11 (16): 2954-2960, 2011
ISSN 1812-5654 / DOI: 10.3923/jas.2011.2954.2960

Extracting Structural Parameters of Nanocrystalline ZnO Thin Films Annealed at Different Temperatures

[1]Gh. Solookinejad and [2]M. Jabbari
[1]Department of Physics, Marvdasht Branch, Islamic Azad University, Marvdasht, Iran
[2]Department of Electronic, Marvdasht Branch, Islamic Azad University, Marvadsht, Iran

Abstract: Preferred orientation of ZnO thin films deposited by sol-gel deposition technique could be manipulated by changing annealing temperature. In this study, we used spin coating method to coat glass slides with sol-gel ZnO thin films, composed of zinc acetate dihydrate Monoethanolamine (MEA), de-ionized water and isopropanol. The effect of the annealing temperature on the structural properties of these films is investigated. These ZnO thin films were preheated at 275°C for 10 min and annealed either at 350, 450 or 550°C for 80 min. After heat treatment, each sample was taken out for *ex situ* Atomic Force Microscopy (AFM) measurements to study the surface morphology. Fractal analysis has been applied to describe the surface morphology and extracting structural parameters of thin films. Thin films also were characterized by X-ray Diffractometery (XRD) method. XRD analysis revealed that the annealed ZnO thin films consist of single phase ZnO with wurtzite structure (JCPDS 36-1451) and show the c-axis grain orientation. Increasing annealing temperature increased the crystallite size and the c-axis orientation of the film after 450°C. It was found that there was a significant effect of annealing temperature on the structural parameters of the film such as roughness exponent, fractal dimension and strain along the c-axis.

Key words: Surface morphology, zinc acetate dihydrate monoethanolamine, annealing temperature, fractal analysis, X-ray diffractometery

INTRODUCTION

Zinc oxide is a wide direct-gap II-VI semiconductor of wurzite structure. It has a direct band gap of 3.37 ev at room temperature which is in ultraviolet rang. However, since the 1960s, preparation of ZnO Thin films has been an active field of study due to application in transducers (Kim *et al*., 2000) and catalysts (Geis *et al*., 1995). Between 1970s and early 1990s, a quasi- two-dimensional form of ZnO was studied roughly for potential application in surface and bulk acoustic ware devices for filtering (Teo *et al*., 2002; Zhu *et al*., 1999) sensing (Dean and Chalamala, 2000; Jo *et al*., 2003) and micromechanical devices like accelerometers, force sensors, tactile sensors and microphones (Jo *et al*., 2004). With an increasing capability of controlling the deposition techniques piezoelectric properties of ZnO thin film were explored (Service, 1997). Since it is transparent in visible light and conductive by doping, ZnO has also been explored as an alternative to Indium Tin oxide (ITO) for display application (Huang *et al*., 2001). In addition to all of these applications, the potential use of ZnO in optoelectronic systems such as Light Emitting Diodes (LED) (Tseng *et al*., 2003), photo detectors (Xu and Sun 2003), electroluminescence devices (Zhu *et al*., 2003), solar cells (Xu *et al*., 2004) and ultraviolet lasers has recently attracted significant attention.

Almost all the surfaces in nature are microscopically rough although they appear to be smooth for naked eye or even for most of the microscopes. All surface properties have become critical in improving the technology on which our modern life is built. For example, semiconductor technology which is backbone of modern technology, involves depositing thin layers of a semiconductor, insulator or metal, then structuring and processing these films with various techniques. In almost all the deposition methods in this technology, self-affine surface gets formed in a growth mode in which average orientation of the surface is maintained but it becomes rough. Surface roughness can affect electrical properties such as electrical capacity, electronic conductivity, surface energy, critical area, peak electric field, surface tension, sheet resistance, etc. (Asenov and Kaya, 2000).

For characterization of thin film surface, Atomic Force Microscopy (AFM) provides very useful numerical data of surface height at digitized locations on a film. Various analyses have been developed to utilize the data,

Corresponding Author: Gh. Solookinejad, Department of Physics, Marvdasht Branch, Islamic Azad University, Marvdasht, Iran

including the root-mean-square of height in wide use, Power Spectrum Density (PSD) (Fang *et al*., 1997) and fractal analyses. These analyses are aiming at finding appropriate morphological parameter (s) to interpret physical properties of the film, or studying the growth mechanism of film, i.e., the 'evolution' of surface morphology.

X-ray Diffraction (XRD) is very widespread and efficient nondestructive tool to investigate the structure and microstructure of bulk as well as surface materials. From the standpoint of thin film X-ray characterization, Grazing Incidence Small Angle X-ray Scattering (GISAXS) is a more recent technique (Levine *et al*., 1989) which combines X-ray Reflectometery (XRR) and transmission mode SAXS theory. XRR and GISAXS studies of sol gel oxide thin films, either alone or in combination, have recently attracted considerable research interest leading to a very rapid increase of the number of published papers and more particularly in the field of sol gel mesoporous thin films (Levine *et al*., 1991).

The influence of substituting low concentration Al at Zn site in ZnO thin films were investigated by Abdullah *et al*. (2009a). Also they simulated single layer Anti-reflective coating on silicon solar cell used on the refractive index limit of Zinc Oxide (Abdullah *et al*., 2009b). The structural and morphological properties of Sn doped ZnO thin films, deposited by spray pyrolysis and chemical bath deposition techniques, were investigated (Baneto *et al*., 2010). The effect of color removal percentage, followed by the effect of ZnO, pH, stirring time and solar photo-catalytic as a final treatment have been investigated by using coagulation as pretreatment (Makhtar *et al*., 2010). Also the effect of CuO content on the microstructure, electrical properties and density of ZnO based varistor ceramics have been investigated (Desouky *et al*., 2010).

In this study, the ZnO thin films were prepared by sol-gel spin coating method and annealed at different temperatures. The effect of annealing temperature on the structural properties of ZnO thin films deposited on microscope glass was investigated by AFM and X-ray.

MATERIALS AND METHODS

Thin film preparation: All the chemicals were analytic grade reagents without further purification and purchased from Merck Company. Nano-crystalline ZnO thin films were prepared on microscope glass slide (75×25×1 mm) substrate (washed with ethanol and dilute acid) by a sol-gel method. Sol solution was prepared by adding 3.10 g Zinc acetate dihydrate ($Zn(CH_3COO)_2 \cdot 2H_2O$: $ZnAc \cdot 2H_2O$), 0.86 g mono-ethanolamine (MEA) and adequate deionized water to 15 mL isopropanol alcohol, then heated to 60°C with continuous stirring for 60 min (Habibi and Sardashti, 2008a). The coating substrate (microscope glass slid) was preheated at 275°C for 10 min in air after each coating. The sol-gel coating was made usually a day after the sol solution was prepared and the molar ratio of MEA to Zinc acetate was maintained at 1:1. Then the films were coated by spin coating method.

The films of ZnO were prepared by spin coating method onto substrate with 3000 rpm for 45 sec (the spinner reached 3000 rpm after 5 sec which was maintained for 40 sec) (Habibi and Sardashti, 2008b). Precursor solution did not produce any precipitation after 30 days. Film deposition was carried out in air at room temperature by a rate 3000 rpm for 30 sec. After each coating, the films were preheated at 275°C for 10 min and post-heated at 350, 450 and 550°C, for 80 min. The deposition was repeated to obtain a film with proper thickness.

X-ray diffraction: X-ray diffraction measurements were carried out in order to study the crystal structure of ZnO thin films. The phase composition of ZnO thin films fabricated by sol-gel spin and dip coating methods were determined using XRD technique with a D8 Advance Bruker X-ray diffractometery at room temperature, with monochromated Cu K_α (λ = 0.154 nm) radiation, in the scan range of 2θ between 25° and 70° with a scan rate of 0.03 deg sec^{-1}.

Atomic force microscopy: *Ex situ* measurements of surface morphology of the films were carried out following heating process. For obtaining surface morphology of thin films we used an Atomic Force Microscopy (AFM) instrument (TM Microscopes Veeco Metrology Group) on contact mode. A commercial standard pyramidal Si3N4 tip was used. AFM images were acquired in ambient air and digitized in to 256*256 pixels. AFM images of ZnO thin films annealed at different temperatures are shown in the Fig. 1a-c.

RESULTS AND DISCUSSION

The concept of fractal dimensionality, in contrast with traditional techniques, has proven very successful both in applying to a wide range of complex surface geometries and in advancing our understanding of how the geometry

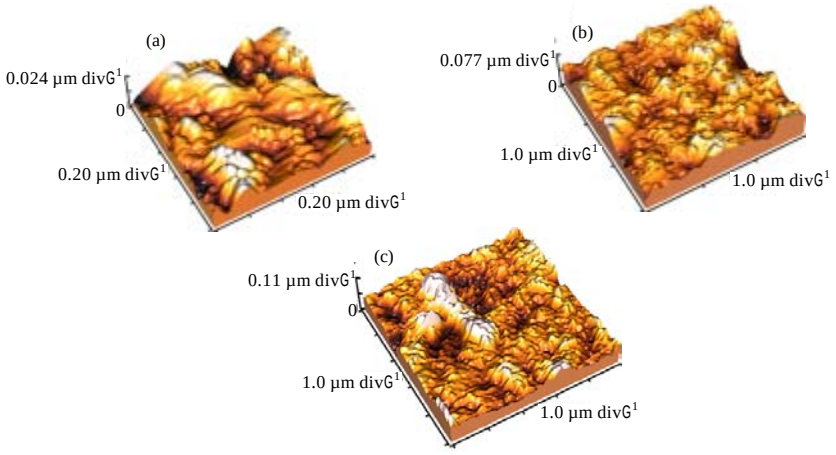

Fig. 1(a-c): AFM images of ZnO thin films annealed at (a) 350, (b) 450 and (c) 550°C

affects the physical properties of the system. In order to study the fractal properties of ZnO thin films, we computed the height-height correlation functions of both samples from AFM images.

Denoting by h (i, j), the height of the surface measured by AFM at the point (i, j), N×N the total number of points at which the surface heights have been measured and d the horizontal distance between two adjacent pixels then the interface width w (or rms) value of the surface roughness is defined as:

$$W = \frac{1}{N}\sqrt{\sum_{i,j=1}^{N}(h(i,j) - \langle h(i,j)\rangle)^2} \quad (1)$$

where, <h (i, j)> is the average overall surface points:

$$\langle h(i,j)\rangle = \frac{1}{N^2}\sum_{i,j=1}^{N} h(i,j)$$

The height-height correlation function H (r) is calculated along the fast scan direction (x direction) through the formula (Ioannou-Sougleridis *et al*., 2004):

$$H(r = md) = \frac{1}{N(N-m)}\sum_{j=1}^{N}\sum_{i=1}^{N-m}[h(i+m,j) - h(i,j)]^2 \quad (2)$$

for self-affine surfaces, the dynamic scaling hypothesis suggests that the height-height correlation function H (r) has the scaling form:

$$H(r) = \begin{cases} r^{2\alpha}, \text{for} \cdots r \prec\prec \xi \\ 2W^2, \text{for} \cdots r \succ\succ \xi \end{cases} \quad (3)$$

where α is the roughness exponent, W is the interface width (rms of surface roughness) and ξ is the lateral correlation length.

Table 1: The rms of roughness, roughness exponents, fractal dimensions and correlation lengths of samples annealed at different temperatures

Annealing temperature (T_{an})	[1]W(nm)	[2]α	[3]D_f	[4]ξ (nm)
350°C	7.1	0.89	2.10	56.2
450°C	18.5	0.35	2.64	354.8
550°C	28.4	0.16	2.83	562.3

[1]rms of roughness, [2]Roughness exponent, [3]Fractal dimension, [4]Correlation length

From height-height correlation function of the surface we can determine the interface width W, the lateral correlation length ξ and the roughness exponent. Figure 2a-c shows the Log of height-height correlation function as a function of Log (r) for ZnO thin films that annealed at different temperatures.

The results of root mean square (rms) of roughness, roughness exponent, fractal dimensions and correlation length for different annealing temperatures that extracted from height-height correlation functions, are summarized in the Table 1. α is the roughness exponent which describes how locally ''wiggly'' the sample surface is, W is the rms of surface roughness and ξ is the lateral correlation length which is defined as the largest distance in which the height is still correlated. The relationship between roughness exponent h and fractal dimension D_f is $D_f = E+1-\alpha$ with $0<\alpha<1$, where E+1 is the dimension of the embedded space. Fractal dimension D_f describes the total profile complexity and takes into account the changes of the normalized profile length as a function of the observation scale. The value of D_f can theoretically change from 2 for a flat profile to 3 for profiles which fill whole area defined by the square constructed by height roughness. If the D_f value is between 2 and 3, then the analyzed profiles have some fractal properties. If the fractal dimension is higher, it suggests that the profile complexity is more pronounced. Also larger value of α corresponds to a locally flat surface structure while a

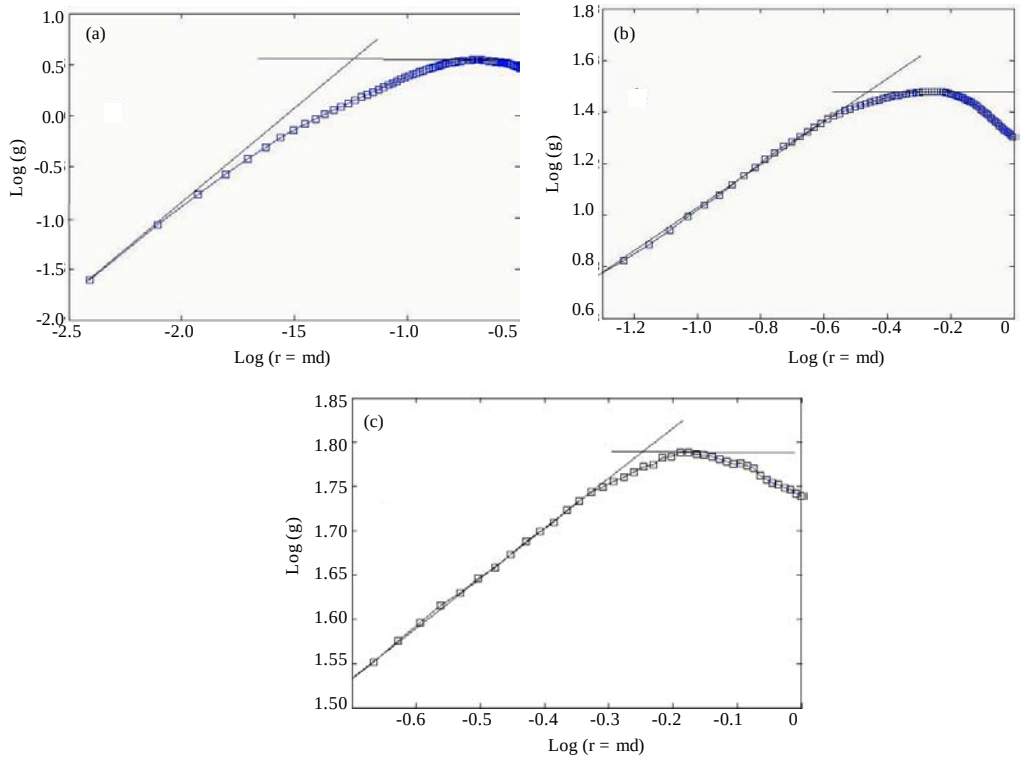

Fig. 2(a-c): Correlation functions of ZnO thin films annealed at (a) 350, (b) 450 and (c) 550°C

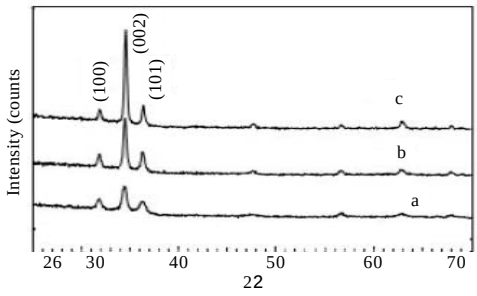

Fig. 3: The XRD pattern of the ZnO thin film on a glass substrate by spin-coating annealed at (a) 350°C, (b) 450°C and (c) 550°C

smaller one corresponds to more locally rough morphology. Surface structural parameters α, W and ξ are independent from each other and they vary according to the process by which the surface morphology is formed. These parameters completely characterize a self-affine surface.

Figure 3 shows the XRD patterns of the ZnO thin film on glass, pre-heated at 275°C and annealed at 350, 450 and 550°C, respectively. It found that the quality of the thin films by sol-gel spin coating process and crystallization was influenced on annealing temperature. Presence of several peaks in all the thin films indicates random orientation of the crystallites. Also, the results clearly show that (002) orientation is preferred when the ZnO films are annealed at 550°C. The preferred c-axis orientation is reported by Wang *et al.* (2006), when the ZnO thin film is annealed at 800°C.

Comparing the XRD patterns of the thin films with ZnO powder showed that thin films have lower intensity and higher FWHM (fully width at half maximum) than the powder and the films are predominantly (002) oriented and films are crystallized at 550°C with highest intensity. Compared to powder diffraction data of zincate (wurzite) structure (JCPDS 36-1451), the XRD patterns of all the films indicated enhanced intensities for the peaks corresponding to (002) plane, indicating preferential orientation along the c-axis. The relative intensity of the peaks corresponding to the (002) plane increased with increasing annealing temperature. The ZnO films grow with a (002) orientation is kinetically preferred which in turn likely reflects the fact that the highest density of Zn atoms is found along the (002) plane (Amirhaghi *et al.*, 1994).

The crystalline size of ZnO in the films was calculated by Scherrer's formula $D = 0.9\lambda/\beta \cos\theta$, where D is the

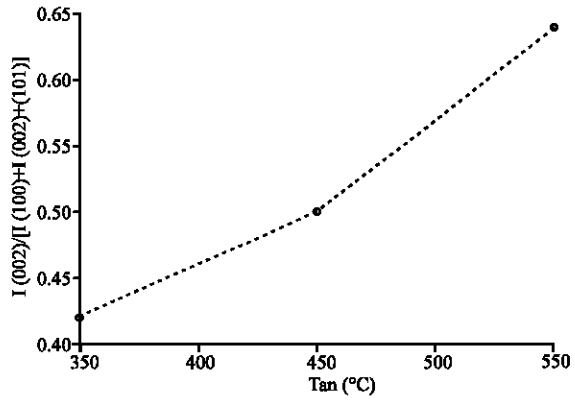

Fig. 4: The relative intensity of (002) peaks vs. annealing temperature (T_{an}) for ZnO thin films

grain size, λ (1.548 °A) is the wavelength of X-ray radiation used, β is the full width at half maximum (FWHM) of the diffraction peak and θ is the Bragg diffraction angle of the XRD peak. The average crystalline size of ZnO in the films annealed at 350, 450 and 550°C was about 19, 22 and 24 nm, respectively. It was observed that the c-axis orientation improves and the grain size increases as indicated by an increase in intensity of the (002) peak and the decrease in the FWHM (Fully Width at Half Maximum) high with the increase of annealed temperature. An average grain size was about 22 nm (Fig. 3).

The relation between relative intensity I(002)/[I(100) +I(002)+I(101)] and annealing temperature (T_{an}) shown in Fig. 4. In view of the fact that c-axis oriented ZnO films were also acquired by using other fabrication methods such as chemical deposition (Kashiwaba *et al*., 2000), Radio Frequency (RF) sputtering (Sundaram and Khan, 1997) and laser ablation (Ryu *et al*., 2000), this fact could be a common aspect in all ZnO thin films. It is believed that the preferential orientation is due to the minimization of surface energy and internal stress (Dinghua *et al*., 1998). Also, the c-orientation might be resulted from the facilitated growth of the film along the c-axis as a result of the highest atomic density found along the (002) plane (Amirhaghi *et al*., 1994).

The lattice parameters can be calculated by using the following formula:

$$d_{hkl} = \frac{1}{\sqrt{4(h^2 + k^2 + hk)/3a^2 + l^2/c^2}} \quad (4)$$

where, a, c are the lattice parameters and d_{hkl} is the crystalline surface distance for h k l indices. First, we have calculated the values of lattice parameters from the X-ray diffraction data and then calculated the values of strain along the c-axis (ε_{zz}) by using the following formula (Ghosh *et al*., 2004):

$$\varepsilon_{zz} = \frac{c - c_0}{c_0} \quad (5)$$

where, c is the lattice parameter of the strained ZnO films calculated from X-ray diffraction data and c_0 (5.207) is the unstrained lattice parameter of ZnO. At the same time, the strain can be negative (compressive) or positive (tensile). The lattice parameters of ZnO thin films, annealed at different annealing temperatures, yield an hexagonal unit cell which are very close to the parameter c_0 = 5.207 A° (Raoufi and Raoufi, 2009).

Table 2: Lattice parameters, relative intensity and strain along the c-axis of (002) peaks of ZnO thin films

Sample	[1]T_{an}(°C)	[2]c	[3]I(002)/[I(100)+I(002)+I(101)]	[4]ε_{zz}
a	350	5.26	0.42	0.0101
b	450	5.18	0.50	-0.005
c	550	5.12	0.64	-0.016
JCPDS	-	5.207	0.2189	-

[1]Annealing temperature, [2]Lattice paremeter, [3]Relative intensity, [4]Strain along the c-axis

As can be seen from Table 2 the heat-treated thin films after 450°C give smaller c values than the ZnO powder. Also this film has the least strain along the c-axis during growth process.

Zhang *et al*. (2006) have also reported slightly smaller c values for nano-crystalline ZnO thin films prepared on p-type Si (1 0 0) substrates by a sol-gel method followed by heat-treatment (Zhang *et al*., 2006). While, Lee *et al*. (2004) have reported slightly higher c values for ZnO thin films prepared on quartz glass substrates by a sol-gel method. The difference in c-axis lattice parameter has to be attributed to the occurrence of stress in the thin films. Under compression (parallel to the surface), the c-axis lattice parameter will decrease, leading to a somewhat larger inter-planar distance for the (002) planes. The mechanism of formation of the c-axis preferentially oriented ZnO thin film can be suggested that the value of the surface free energy is the least for the ZnO (002) plane at the growth stage.

CONCLUSION

Glass plate-supported nanostructure ZnO thin films were deposited by sol-gel spin coating. Films were preheated at 275°C for 10 min and annealed at 350, 450 and 550°C for 80 min. The effect of annealing temperatures on the quality characteristics of ZnO thin films was studied. XRD pattern of ZnO thin films showed polycrystalline wurtzite with a preferential (002) orientation. Increasing

annealing temperature increased the crystallite size of the thin film and the c-axis orientation after 450°C. Using fractal analysis of AFM data for extracting surface parameters of ZnO thin films at different temperatures showed that, increasing annealing temperature increased lateral correlation length, fractal dimension and rms of roughness. These results suggest that increasing annealing temperature produces jagged thin film and this film can be used for photo-catalytic applications.

ACKNOWLEDGMENTS

The authors would like to thank the Office of Graduate Studies of the University of Isfahan for their support. Gh. Solookinejad would like to thank the Iranian Nanotechnology Initiative Council for their support.

REFERENCES

Abdullah, H., A. Lennie and I. Ahmad, 2009a. Modelling and simulation single layer anti-reflective coating of ZnO and ZnS for silicon solar cells using silvaco software. J. Applied Sci., 9: 1180-1184.

Abdullah, H., R. Silvia and J. Syarif, 2009b. Study of structure, surface morphology and optical property on ZnO: Al thin films as anti-reflecting coating. Asian J. Applied Sci., 2: 191-196.

Amirhaghi, S., V. Craciun, D. Craciun, J. Elders and I.W. Boyd, 1994. Low temperature growth of highly transparent c-axis oriented ZnO thin films by pulsed laser deposition. Microelectron. Eng., 25: 321-326.

Asenov, A. and S. Kaya, 2000. Effect of oxide interface roughness on the threshold voltage fluctuations in decanano MOSFETs with ultrathin gate oxides. Proceedings of the International Conference on Simulation of Semiconductor Processes and Devices, Sept. 6-8, Seattle, Washington, pp: 135-138.

Baneto, M., Y. Lare, L. Cattin, M. Addou and K. Jondo *et al*., 2010. Comparison of the structural and morphological properties of Sn doped ZnO films deposited by spray pyrolysis and chemical bath deposition. Asian J. Mater. Sci., 2: 196-203.

Dean, K.A. and B.R. Chalamala, 2000. Current saturation mechanisms in carbon nanotube field emitters. Appl. Phys. Lett, 76: 375-375.

Desouky, O.A., S.M. Negim, W.A. Kamil and S.E. Mansour, 2010. Microstructure and Current-voltage Characteristics of (ZnO-CuO) varistor system in the presence of additive oxides, Cr_2O_3, Bi_2O_3 and NiO. Curr. Res. Chem., 2: 1-9.

Dinghua, B., H. Gu and A. Kuang, 1998. Sol-gel-derived c-axis oriented ZnO thin films. Thin Solid Films, 312: 37-39.

Fang, S.J., S. Haplepete, W. Chen, C.R. Helms and H. Edwards, 1997. Analyzing atomic force microscopy images using spectral methods. J. Appl. Phys., 82: 5891-5898.

Geis, M. W., J. C. Twichell, J. Macaulay and K. Okano, 1995. Electron field emission from diamond and other carbon materials after H_2, O_2 and Cs treatment. Appl. Phys. Lett., 67: 1328-1330.

Ghosh, R., D. Basak and S. Fujihara, 2004. Effect of substrate-induced strain on the structural, electrical and optical properties of polycrystalline ZnO thin films. J. Appl. Phys., 96: 2689-2689.

Habibi, M.H. and M.K. Sardashti, 2008a. Preparation of glass plate-supported nanostructure ZnO thin film deposited by sol-gel spin-coating technique and its photocatalytic degradation to monoazo textile dye. J. Nanomater., 2008: 1-5.

Habibi, M.H. and M.K. Sardashti, 2008b. Structure and morphology of nanostructured zinc oxide thin films prepared by Dipvs. spin-coating methods. J. Iran. Chem. Soc., 5: 603-609.

Huang, M.H., S. Mao, H. Feick, H. Yan and Y. Wu *et al*., 2001. Room-temperature ultraviolet nanowire nanolasers. Science, 292: 1897-1899.

Ioannou-Sougleridis, V., V. Constantoudis, M. Alexe, R. Scholz, G. Vellianitis and A. Dimoulas, 2004. Effects on surface morphology of epitaxial Y_2O_3 layers on Si (001) after postgrowth annealing. Thin Solid Films, 468: 303-309.

Jo, S.H., Y. Tu, Z.P. Huang, D.L. Carnahan, D.Z. Wang, Z.F. Ren, 2003. Effect of length and spacing of vertically aligned carbon nanotubes on field emission properties. Appl. Phys. Lett., 82: 3520-3522.

Jo, S.H. Y. Tu, Z.P. Huang, D.L. Carnahan, J.Y. Huang, D.Z. Wang and Z.F. Ren, 2004. Correlation of field emission and surface microstructure of vertically aligned carbon nanotubes. Appl. Phys. Lett., 84: 413-415.

Kashiwaba, Y., F. Katahira, K. Haga, T. Sekiguchi and H. Watanabe, 2000. Hetero-epitaxial growth of ZnO thin films by atmospheric pressure CVD method. J. Cryst. Growth, 122: 431-434.

Kim, J.M., W.B. Choi, N.S. Lee and J.E. Jung, 2000. Field emission from carbon nanotubes for displays. Diam. Relat. Mater., 9: 1184-1189.

Lee, H.S., J.Y. Lee, T.W. Kim, D.W. Kim and W.J. Cho, 2004. Formation mechanism of preferential *c*-axis oriented ZnO thin films grown on p-Si substrates. J. Mater. Sci., 39: 3525-3528.

Levine, J.R., J.B. Cohen, Y.W. Chung and P. Georgopoulos, 1989. Grazing-incidence small-angle X-ray scattering: new tool for studying thin film growth. J. Appl. Crystallogr, 22: 528-532.

Levine, J.R., J.B. Cohen and Y.W. Chung, 1991. Thin film island growth kinetics: A grazing incidence small angle X-ray scattering study of gold on glass. Surf. Sci., 248: 215-224.

Makhtar, S.M.Z., N. Ibrahim and M.T. Selimin, 2010. Removal of colour from landfill by solar photocatalytic. J. Applied Sci., 10: 2721-2724.

Raoufi, D. and T. Raoufi, 2009. The effect of heat treatment on the physical properties of sol-gel derived ZnO thin films. Appl. Surf. Sci., 255: 5812-5817.

Ryu, Y.R., W.J. Kim and H.W. White, 2000. Fabrication of homostructural ZnO pn junctions. J. Cryst. Growth, 219: 419-422.

Service, R.F., 1997. Will UV lasers beat the blues? Science, 276: 895-895.

Sundaram, K.B. and A. Khan, 1997. Characterization and optimization of zinc oxide films by r.f. magnetron sputtering. Thin Solid Films, 295: 87-91.

Teo, K.B.K. and M. Chholwalla, G.A.J. Amaratunga, W.I. Milne and G. Priro *et al*., 2002. Field emission from dense, sparse and patterned arrays of carbon nanofibers. Appl. Phys. Lett., 80: 2011-2013.

Tseng, Y.K., C.J. Huang, H.M. Cheng, I.N. Lin, K.S. Liu, I.C. Chen, 2003. Characterization and field emission properties of needle like zinc oxide nanowires grown vertically on conductive zinc oxide films. Adv. Func. Mater., 13: 811-814.

Wang, M., J. Wang, W. Chen, Y. Cui and L. Wang, 2006. Effect of preheating and annealing temperatures on quality characteristics of ZnO thin film prepared by sol-gel method. Mater. Chem. Phys., 97: 219-225.

Xu, C.X. and X.W. Sun, 2003. Field emission from zinc oxide nanopins. Applied Phys. Lett., 83: 3806-3808.

Xu, C.X., X.W. Sun and B.J. Chen, 2004. Field emission from gallium-doped zinc oxide nanofiber array. Applied Phys. Lett., 84: 1540-1542.

Zhang, Y., B. Lin, Z. Fu, C. Liu and W. Han, 2006. Strong ultraviolet emission and rectifying behavior of nanocrystalline ZnO films. Opt. Mater., 28: 1192-1196.

Zhu, W., C. Bower, O. Zhou, G. Kochanski and S. Jin, 1999. Large current density from carbon nanotube field emitters. Applied Phys. Lett., 75: 873-875.

Zhu, Y.W., H.Z. Zhang, X.C. Sun, S.Q. Feng and J. Xu *et al*., 2003. Efficient field emission from ZnO nanoneedle arrays. Applied Phys. Lett., 83: 144-146.